EPJ manuscript No.
(will be inserted by the editor)

Non-perturbative gluonic dressing effect of extended scalar diquark in the Schwinger-Dyson formalism

Shotaro Imai[1] and Hideo Suganuma[2]

[1] Faculty of Science, Hokkaido University, Sapporo 060-0810, Japan e-mail: imai@nucl.sci.hokudai.ac.jp
[2] Department of Physics, Graduate School of Science, Kyoto University, Kitashirakawa-oiwake, Sakyo, Kyoto 606-8502, Japan e-mail: suganuma@ruby.scphys.kyoto-u.ac.jp

arXiv:1401.7762v2 [hep-ph] 26 Aug 2015

Received: date / Revised version: date

Abstract. In terms of the structure of exotic hadrons and heavy hadronic states, diquarks have been considered as important effective degrees of freedom. The diquark is composed of two quarks with gluonic interaction, and it still strongly interacts with gluons because of its non-zero color charge. We investigate the gluonic dressing effect for a scalar diquark using the Schwinger-Dyson formalism in the Landau gauge. The scalar diquark is treated as an extended fundamental field like a meson in effective hadron models. The Schwinger-Dyson equation for the scalar diquark diagrammatically has an additional 4-point interaction term, in comparison with the single quark case. Here, we introduce an effective size of the diquark inside a hadron, since it is a bound-state-like object of two quarks. The effective size and the bare mass of the diquark are free parameters in this scalar theory. The diquark effective size R can be taken to be smaller than a hadron, $R \sim 1$ fm, and larger than a constituent quark, $R \sim 0.3$ fm. The bare mass is considered as twice of constituent quark mass or twice of running quark mass, which is determined by the Schwinger-Dyson equation for single quark. We find that the compact diquark with $R \simeq 0.3$ fm has a large effective mass about 900 MeV in both cases of bare mass, and therefore such a compact diquark is not acceptable in effective models for hadrons. We also consider the artificial removal of 3- and 4-point interaction, respectively, to see the role of each term, and find that the 4-point interaction plays the dominant role of the diquark self-energy. Finally, we discuss the non-chiral origin mass generation mechanism of scalar diquark by non-perturbative gluonic dressing effect.

PACS. 12.38.Aw General properties of QCD (dynamics, confinement, etc.) – 12.40.-y Other models for strong interactions – 14.65.-q Quarks – 14.70.Dj Gluons

1 Introduction

Description of hadron structure and its properties are fundamental problems of quantum chromodynamics (QCD). Quarks and gluons, which are ingredients of QCD, are confined and strongly interact with each other in a hadron. Due to the non-perturbative property of QCD, it is difficult to identify that they are effective degrees of freedom of components of hadrons. The constituent quark model picture gives us the hadrons are constructed by some of valence quarks and antiquarks with a sea of gluons and quark/antiquark pairs. The constituent quarks belong to the fundamental representation $\mathbf{3}_c$ in the SU(3) color group, and the color singlet states $\mathbf{1}_c$ can be observed. Three quarks compose baryons and quark/antiquark pair compose mesons. The quark model has been successfully used to describe the hadron spectroscopy. However, QCD allows the existence of other color singlet states, which are not classified into ordinary baryons and mesons, such as glueballs, hybrids and multi-quark states, called exotic hadrons. Recent experiments have reported the candidates for these exotic states [1]. The heavy hadron which includes one or more heavy (anti)quarks is also a recent hot topic in hadron spectroscopy [1,2,3].

In the theoretical study of these states, the diquark picture [4,5] is discussed as an important effective degree of freedom. The diquark is composed of two quarks with strong correlation, where the one gluon exchange interaction between two quarks is attractive in the color anti-triplet $\bar{\mathbf{3}}_c$ channel [6,7], of which color is the same as an anti-quark. In SU(3) flavor case, the flavor antisymmetric and spin singlet with even parity is the most attractive channel in diquark, which is called scalar diquark. If the diquark correlation is developed in a hadron, this scalar diquark channel would be favored. The diquark correlation in a hadron is discussed in various situations, such as tetra-quarks, heavy baryons and other exotic states [8,9]. The tetra-quark states as the bound state of the diquark/antidiquark is suggested in early day [10], and X(3872) [11] and X(1576) [12] are considered as tetraquark states. Light flavor mesons as tetra-quark [13,14, 15,16,17,18,19,20,21,22] and mixing with $q\bar{q}$ state [23,

24,25] are discussed. There are various studies the heavy baryons focused on diquark [26,27,28,29,30], e.g., single heavy quark/light diquark (Qqq) picture [31,32,33,34,35]. The other exotic states including heavy quark(s) are studied [36,37,38,39,40,41,42]. The ordinary baryon properties focused on the diquarks have been also discussed [43, 44,45,46,47]. The diquark correlation is found in the lattice QCD simulation [48,49,50,51]. It is also considered that the diquark condensation is occurred in an extremely high density system, called the color superconductivity [52]. We note that diquark properties strongly depend on the color number N_c. If we consider the two-color QCD, the diquarks compose the color singlet (baryons). The strength of correlation between two quarks is same as quark/antiquark channel, and the (diquark-)baryons correspond to the mesons. This fact is known as the Pauli-Gürsey symmetry. The quark-hadron matter in two-color system is investigated [53, 54,55,56,57,58,59]. For the $N_c = 4$ case, the diquarks belong to $\mathbf{6}_c$ or $\mathbf{10}_c$. As an interesting fact for the case, the diquark contents must be different between baryons and tetra-quarks. In fact, the diquark qq in an $N_c = 4$ baryon $qqqq$ belongs to $\mathbf{6}_c$, which is self-adjoint. On the other hand, the diquark in a tetra-quark $qq\bar{q}\bar{q}$ belongs to $\mathbf{10}_c$. From this viewpoint, the $N_c = 3$ case is rather special, because the diquarks belong to the same color $\bar{\mathbf{3}}_c$ in both cases of baryon qqq and tetra-quark $qq\bar{q}\bar{q}$.

The properties of diquarks such as the mass and size are not understood well, although the diquarks have been discussed as important object of hadron physics. While the diquark is made by two quarks with gluonic interaction, it still strongly interacts with gluons additionally because of its non-zero color charge. Therefore, such dressing effect of gluons for diquark should be considered in a non-perturbative way. The dynamics of diquark and gluons may affect the structure of hadrons. In the quark-hadron physics, the Schwinger-Dyson (SD) formalism is often used to evaluate the non-perturbative effect based on QCD [60,61,62,63,64,65,66,67,68,69,70]. In this paper, we apply the SD formalism to scalar diquark to investigate the effective mass of scalar diquark, which reflects a non-perturbative dressing effect by gluons. The scalar diquark is treated as an extended fundamental field like a meson in effective hadron models, and interacts with the gluons [32,71].

For the argument of the scalar diquark, it would be important to consider its effective size. For, point scalar particles generally have large radiative corrections even in the perturbation theory [72,73]. As an example, in the framework of the grand unified theory (GUT), the Higgs scalar field suffers from a large radiative correction of the GUT energy scale, and therefore severe "fine-tuning" is inevitably required to realize the low-lying Higgs mass of about 126GeV [74], which leads to the notorious hierarchy problem [72,73]. The Higgs propagator with radiative correction has been investigated by setting the mass renormalization condition to reproduce 126 GeV [75,76,77]. A similar large radiative correction also appears for pointlike scalar-quarks, which correspond to compact scalar diquarks, in scalar lattice QCD calculations [71]. In fact, the pointlike scalar-quark interacting with gluons acquires a large extra mass of about 1.5 GeV at the cutoff $a^{-1} \simeq 1$ GeV, where a is the lattice spacing. Such a large-mass acquirement would be problematic in describing hadrons with scalar diquarks. However, since it is a bound-state-like object inside a hadron, the diquark must have an effective size. This effective gives a natural UV cutoff of the theory, and reduces the large radiative correction. Then, we take account of the effective size and investigate the mass of the scalar diquark inside a hadron within the SD formalism.

As for the mass, it is considered that the origin of masses of light sector quarks are generated by the spontaneous chiral symmetry breaking except for a few MeV current mass. We can see that QCD has several dynamical mass generation mechanism, even without chiral symmetry breaking. For example, while the charm quark has no chiral symmetry, some difference seems to appear between current and constituent masses for charm quarks: the current mass is $m_c \simeq 1.2$ GeV at renormalization point $\mu = 2$ GeV [1], and the constituent charm quark mass is $M_c \simeq 1.6$ GeV in the quark model. The gluon is more drastic case. While the gluon mass is zero in perturbation QCD, the non-perturbative effect of the self-interaction of gluons seems to generate a large effective mass of 0.6 GeV [78,79,80], and the lowest glueball mass is about 1.6GeV [81,82]. Furthermore, the dynamical mass generation for scalar-quark have been studied in the scalar lattice QCD calculation [71].

This paper is organized as follows. In Sec. 2, we briefly review the SD formalism for the single quark to set up the formalism for the scalar diquark case. The SD equation for the scalar diquark is discussed in Sec. 3, and we introduce a simple form factor to consider the size of diquark. In Sec. 4, we present the numerical result of the diquark self-energy with the dependence of the bare mass and size of diquark. The dynamical mass generation for the scalar diquark in the SD formalism is discussed in Sec. 5. Section 6 is devoted to conclusion and discussion.

2 The Schwinger-Dyson Equation for the Single Quark (basic formalism)

In this section, we explain the Schwinger-Dyson (SD) formalism for the single quark. The basic formalism, discussed in this section, will be used in the scalar diquark case. The dressed quark propagator is obtained by solving the SD equation as $S(p^2) = iZ(p^2)(\not{p} - \Sigma_q(p^2))^{-1}$ with the wave function renormalization $Z(p^2)$ and the self-energy of quark $\Sigma_q(p^2)$ in the Minkowski space. We assume the rainbow-ladder approximation, where the non-perturbative effect of gluons is included in the dressed quark-gluon vertex $\Gamma^\mu_a(p,k)$. By improving the momentum dependence of the quark-gluon vertex in the one-loop level renormalization-group, the quark-gluon vertices in

the diagram Fig. 1 is rewritten as

$$\frac{g^2}{4\pi} Z_g((p-k)^2)\gamma^\mu T_a \Gamma_b^\nu(p,k) \to \alpha_s((p-k)^2)\gamma^\mu T_a \gamma^\nu T_b, \tag{1}$$

where $Z_g((p-k)^2)$ is the gluon dressing function and $T_a (a = 1, \cdots, 8)$ is the generator of color group. The

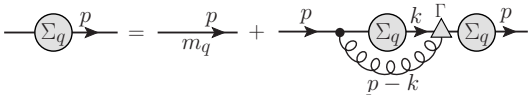

Fig. 1. The Schwinger-Dyson equation for the single quark. The shaded blob denotes the self-energy of quark $\Sigma_q(p^2)$, the black dot the bare quark-gluon vertex, the shaded triangle the dressed vertex $\Gamma_a^\mu(p,k)$, the solid line the quark propagator and the curly line the gluon propagator.

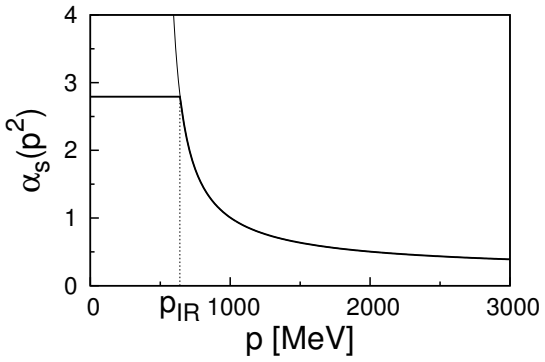

Fig. 2. The behavior of the running coupling of our model $\alpha_s(p^2)$ as a function of the momentum p in the Euclidean space. The thin line is the one-loop renormalization group improved running coupling. We introduce a simple cut at $p_{\rm IR}$ as an infrared regularization.

Higashijima-Miransky approximation, which is to take the maximum value of the argument in the coupling as $\alpha_s((p_E - k_E)^2) \approx \alpha_s(\max(p_E^2, k_E^2))$ in the Landau gauge is used in this study. Here, p_E denotes the Euclidean space momentum. We use a renormalization-group-improved coupling in the case of $N_c = 3$ and $N_f = 3$,

$$\alpha_s(p_E^2) = \frac{g^2(p_E^2)}{4\pi} = \begin{cases} \frac{12\pi}{11N_c - 2N_f} \frac{1}{\ln(p_E^2/\Lambda_{\rm QCD}^2)} & (p_E^2 \geq p_{\rm IR}^2) \\ \frac{12\pi}{11N_c - 2N_f} \frac{1}{\ln(p_{\rm IR}^2/\Lambda_{\rm QCD}^2)} & (p_E^2 \leq p_{\rm IR}^2) \end{cases} \tag{2}$$

with an infrared regularization of a simple cut at $p_{\rm IR} \simeq 640$ MeV which leads to $\ln(p_{\rm IR}^2/\Lambda_{\rm QCD}^2) = 1/2$, and the QCD scale parameter $\Lambda_{\rm QCD} = 500$ MeV [64,65,69]. The infrared regularization has been introduced to avoid the divergent pole at $p = \Lambda_{\rm QCD}$. The scale parameter $\Lambda_{\rm QCD}$ is chosen to reproduce chiral properties for quarks in the SD formalism with the Higashijima-Miransky approximation in the Landau gauge (see Eqs. (5)–(7)), while the ordinary QCD scale parameter is around $\Lambda_{\rm QCD} \sim 200 - 300$ MeV. The behavior of the coupling is shown in Fig. 2 in the Euclidean space. We will show all the figures are in the Euclidean space, except for the figures 1, 4, 5 and 10. In the Landau gauge, the gluon propagator is written as

$$D_{\mu\nu}^{ab}(p^2) = \frac{-1}{p^2}\left(g_{\mu\nu} - \frac{p_\mu p_\nu}{p^2}\right)\delta^{ab}, \tag{3}$$

and the wave function renormalization can be taken as $Z(p^2) = 1$.

The quark self-energy $\Sigma_q(p_E^2)$ is determined by solving the SD equation,

$$\begin{aligned}\Sigma_q(p_E^2) =& m_q + \frac{3C_2(\mathbf{3})}{4\pi^3}\int d^4k_E \frac{\alpha_s((p_E-k_E)^2)}{(p_E-k_E)^2}\frac{\Sigma_q(k_E^2)}{k_E^2+\Sigma_q^2(k_E^2)} \\ =& m_q + \frac{2\alpha_s(p^2)}{\pi p_E^2}\int_0^{p_E} dk_E \frac{k_E^3\Sigma_q(k_E^2)}{k_E^2+\Sigma_q^2(p_e^2)} \\ &+ \frac{2}{\pi}\int_{p_E}^{\Lambda_{\rm UV}} dk_E \frac{k_E\alpha_s(k_E^2)\Sigma_q(k_E^2)}{k_E^2+\Sigma_q^2(k_E^2)},\end{aligned} \tag{4}$$

where the Wick rotation has been taken and the Casimir operator $C_2(\mathbf{3}) = \sum_{a=1}^8 T^a T^a = 4/3$ obtained by the color trace. The result of the SD equation is shown in Fig. 3 in the chiral limit $m_q = 0$. There is a small cusp structure at $p_{\rm IR}$ due to the coupling behavior Eq. (2). The ultraviolet cutoff $\Lambda_{\rm UV}$ is taken as 5 GeV. The self-energy $\Sigma_q(p_E^2)$ is unchange even the cutoff is taken 10 GeV. The quark mass is large at the infrared region and monotonously goes to zero with the momentum, which reflects the spontaneous chiral symmetry breaking [63,64,83,84].

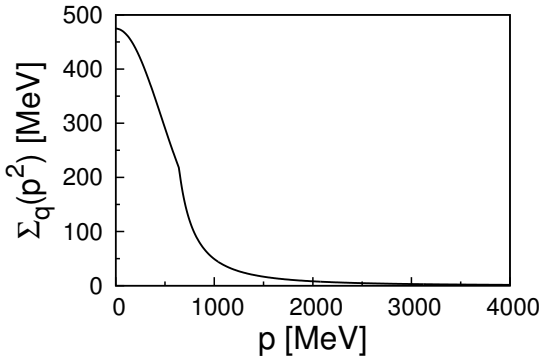

Fig. 3. The quark self-energy $\Sigma_q(p^2)$ as a function of the momentum p in the chiral limit. The self-energy is large in the low momentum region and goes to zero monotonously with the momentum.

The self-energy leads to the pion decay constant with the Pagels-Stokar approximation [85]:

$$\begin{aligned} f_\pi^2 =& \frac{N_c}{2\pi^2}\int_0^\infty dk_E \frac{k_E^3\Sigma_q(k_E^2)}{k_E^2+\Sigma_q^2(k_E^2)} \\ &\times\left(\Sigma_q(k_E^2) - \frac{k_E}{4}\frac{d}{dk_E}\Sigma_q(k_E^2)\right),\end{aligned} \tag{5}$$

and the (unrenormalized) chiral condensate:

$$\langle\bar{q}q\rangle_{\Lambda_{\rm UV}} = -\frac{N_c}{2\pi^2}\int_0^{\Lambda_{\rm UV}} dk_E \frac{k_E^3\Sigma_q(k_E^2)}{k_E^2+\Sigma_q^2(k_E^2)}. \quad (6)$$

Since the pion decay constant is a physical value, its renormalization is not required and it does not depend on the ultraviolet cutoff $\Lambda_{\rm UV}$. Hence, the upper limit of the integration has been taken as $\Lambda_{\rm UV}\to\infty$. On the other hand, the chiral condensate depends on the renormalization point. We adopt a standard renormalization point $\mu = 2$ GeV [1], and consider the chiral condensate $\langle\bar{q}q\rangle_{\mu=2\rm GeV}$ according to the renormalization-group formula [65,66,69]:

$$\langle\bar{q}q\rangle_{\mu=2\rm GeV} = \left(\frac{\alpha_s(\Lambda^2)}{\alpha_s(\mu^2)}\right)^{\frac{3C_2(N_c)}{16\pi^2\beta_0}} \langle\bar{q}q\rangle_{\Lambda_{\rm UV}}, \quad (7)$$

with $\frac{3C_2(N_c)}{16\pi^2\beta_0} = 4/9$ and $\beta_0 = \frac{11N_c-2N_f}{48\pi^2}$ corresponding to the lowest coefficient of the β function of the renormalization group. Taking the scale parameter $\Lambda_{\rm QCD}$ as 500 MeV [64,65,69] and the ultraviolet cutoff $\Lambda_{\rm UV}$ as 5 GeV, the pion decay constant and the chiral condensate are fixed as $f_\pi \simeq 90$ MeV and $-\langle\bar{q}q\rangle^{1/3}_{\mu=2\rm GeV} \simeq 242$ MeV, respectively. We have numerically checked that they are stable against the variation of the ultraviolet cutoff $\Lambda_{\rm UV}$. The SD formalism with the approximations in the Landau gauge reproduces these chiral properties well.

3 The Schwinger-Dyson Equation for the Scalar Diquark

Diquark is a bound-state-like object of two quarks and decomposed into color anti-triplet $\bar{\mathbf{3}}_c$ and sextet $\mathbf{6}_c$ and flavor anti-triplet $\bar{\mathbf{3}}_f$ and sextet $\mathbf{6}_f$ in SU(3) flavor case. The most attractive channel for diquark is the color and flavor anti-triplet $\bar{\mathbf{3}}_{c,f}$ and spin singlet with even parity 0^+ by one gluon exchange [6,7] and by instanton interactions [86,87], which is called scalar diquark. If the diquark correlation is developed in a hadron such as a heavy baryon (Qqq), this scalar diquark channel would be favored. We consider the scalar diquark as an effective degree of freedom with a peculiar size, assuming it to be an extended fundamental field $\phi(x)$ [32,71] like a meson in the effective hadron models. The scalar diquark is composed of two quarks with the gluonic interaction, and still affected by non-perturbative gluonic effects since it has non-zero color charge as shown Fig. 4. The dynamics of the scalar diquark field ϕ is described by the gauge-invariant Lagrangian:

$$\mathcal{L} = [(\partial^\mu + igA_a^\mu T^a)\phi]^\dagger[(\partial_\mu + igA_{\mu b}T^b)\phi] - m_\phi^2\phi^\dagger\phi, \quad (8)$$

where the bare diquark mass m_ϕ and the gauge field A_a^μ (gluon) with the generator T^a have been introduced. We note that the scalar diquark has the 4-point interaction term of $|\phi|^2A^2$ type, which is different from the quark. In general, such gauged scalar fields accompany the 4-point interaction [72,75,76,77,88].

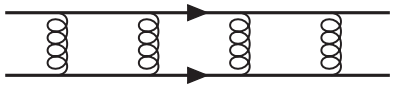

(a) The gluonic interaction between two quarks

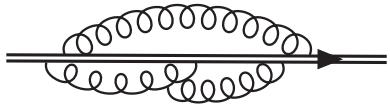

(b) The gluonic dressing for a diquark

Fig. 4. The two types of gluonic interaction for a diquark: (a) inter-two-quarks gluonic interaction to form a diquark and (b) gluonic dressing for the diquark due to its non-zero color charge. The single line denotes a quark, the double line a diquark and the curly line a gluon.

Since the diquark is confined and located in a hadron, the diquark must have an effective size smaller than the hadron. In order to include the size effect of diquark, we introduce a simple "form factor" in the 4D Euclidean space as

$$f_\Lambda(p_E^2) = \left(\frac{\Lambda^2}{p_E^2+\Lambda^2}\right)^\nu, \quad (9)$$

where the momentum cutoff Λ corresponds to the inverse of the diquark size R. In this paper, we set $R \equiv \Lambda^{-1}$. Since the radiative correction for the scalar particle is generally large, this form factor has also a role of the convergence factor. As for the form factor $f_\Lambda(p_E^2)$, it has the roles of introducing an effective size and convergence of the SD equation, so one can use arbitrary function such as the step function $\theta(\Lambda^2-p_E^2)$, the exponential function $\exp(-p_E^2/\Lambda^2)$ and so on. In this study, we take Eq. (9) with $\nu = 2$ to simple analysis and the convergence of the SD equation. The size effect of the diquark can be included in the vertex as $\alpha_s(p^2)\to\alpha_s(p^2)f_\Lambda(p^2)$.

While the scalar QCD Lagrangian (8) is renormalizable, this theory is an effective cutoff theory with an UV cutoff parameter Λ, which corresponds to the inverse size of the scalar diquark. Here, the scalar diquark cannot be observed as an isolated object, and has no characteristic symmetry, such as the chiral symmetry, so that it is difficult to set the renormalization condition. Instead, we introduce an effective size $R = \Lambda^{-1}$ of the diquark, which leads to a natural UV cutoff in the theory. As we will see later, the effective size of diquark will play an important role for the convergent of loop integrations, and therefore we will not take the limit of $\Lambda\to\infty$ ($R\to 0$).

We now describe the SD equation for the scalar diquark, as shown in Fig. 5. For the self-energy diagram, we include the first order of the coupling α_s at the one-loop level, like the improved ladder QCD [63,64,65,66]. Note however that, due to the iterative calculation, this formalism includes infinite order of the coupling α_s and describes non-perturbative effects. Basically, we use the same framework as the single quark case, which is discussed in the previous section such as the running cou-

pling and parameters, for the scalar diquark case. It is notable that we can use the same form of the running coupling for quark/gluon coupling even for the scalar diquark/gluon [89,90]. The origin of the running coupling comes from the renormalization-group analysis. In the heavy mass limit of interacting particles, the interaction depends on only color. Since the scalar diquark corresponds to the antiquark in the color group, we may use same form of the running coupling even for the scalar diquark case. The SD equation for the scalar diquark is diagrammatically expressed as Fig. 5 and is written by

$$\begin{aligned}\Sigma^2(p_E^2) =& m_\phi^2 + \frac{3C_2(\mathbf{3})}{2\pi^3}\int_0^{\Lambda_{\rm UV}} d^4k_E \frac{\alpha_s(k_E^2)f_\Lambda(k_E^2)}{k_E^2} \\ & -\frac{C_2(\mathbf{3})}{4\pi^3}\int_0^{\Lambda_{\rm UV}} d^4k_E \frac{\alpha_s((p_E-k_E)^2)f_\Lambda((p_E-k_E)^2)}{k_E^2+\Sigma^2(k_E^2)} \\ & \times \frac{4p_E^2k_E^2-4(p_E\cdot k_E)^2}{(p_E-k_E)^4} \\ =& m_\phi^2 + \frac{4}{\pi}\int_0^{\Lambda_{\rm UV}} dk_E k_E \alpha_s(k_E^2)f_\Lambda(k_E^2) \\ & -\frac{2\alpha_s(p_E^2)f_\Lambda(p_E^2)}{\pi p_E^2}\int_0^{p_E} dk_E \frac{k_E^5}{k_E^2+\Sigma^2(k_E^2)} \\ & -\frac{2}{\pi}\int_{p_E}^{\Lambda_{\rm UV}} dk_E \frac{\alpha_s(k^2)f_\Lambda(k_E^2)k_E}{k_E^2+\Sigma^2(k_E^2)}. \end{aligned} \tag{10}$$

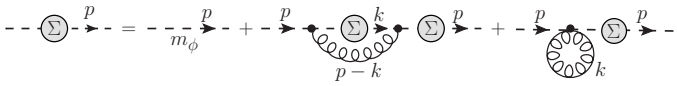

Fig. 5. The Schwinger-Dyson equation for the scalar diquark. The shaded blob is the self-energy $\Sigma(p^2)$, the dashed line denotes the scalar diquark propagator and the curly line the gluon propagator. The last term (4-point interaction) is the peculiar term of scalar theory, which does not appear in the single quark case.

The second term corresponds to the 4-point interaction term and the third term is the 3-point interaction term in Fig. 5. Here, we do not consider the wave functional renormalization, since the diquark is confined in a hadron and do not produce any physical quantities. The physical quantities will be discussed in the color singlet state such as heavy baryons, which is our future work.

4 Numerical Result

4.1 The parameter setting

The bare mass m_ϕ and cutoff Λ (inverse of the size R) are free parameters of the diquark theory. In this subsection, we consider the possible range of these parameters from the physical viewpoint.

The diquark is originally made of two consistent quarks, and the color-Coulomb interaction is one of the main attractive forces. We here estimate the color-Coulomb interaction between the two massive quarks from the three-quark (3Q) potential [95], or generally from the mult-quark potential such as $4\bar{\rm Q}({\rm QQ\bar{Q}\bar{Q}})$ and $5{\rm Q}(4\bar{\rm Q})$ potentials [96]. In SU(3) lattice QCD, the 3Q potential among the three quarks located at $\mathbf{r}_i (i=1,2,3)$ is well reproduced by

$$V_{\rm 3Q} = -\sum_{i<j}\frac{A_{\rm 3Q}}{|\mathbf{r}_i-\mathbf{r}_j|} + \sigma L_{\rm min}, \tag{11}$$

with the color-Coulomb coefficient $A_{\rm 3Q} \simeq A_{\rm Q\bar{Q}}/2 \simeq 0.12(1)$, the string tension $\sigma \simeq 0.89$GeV/fm and the minimal flux-tube length $L_{\rm min}$ [95]. Since the color-Coulomb potential energy between two quarks is $A_{\rm 3Q}/R$ for the inter-quark distance R, the potential energy is estimated as $A_{\rm 3Q}/R \simeq 24-80$MeV for the typical range of $R=0.3-1$fm, and its value is not so large in comparison with the two-quark mass of about 600MeV. [Note also that similar estimation also leads to a small value of the diquark-diquark interaction, which gives a reason of the absence of $(\phi^\dagger\phi)^2$ in the diquark Lagrangian (8).] The same result can be obtained from the multi-quark potential [96], because the color-Coulomb coefficient is the same for two quarks in the diquark, i.e., $A_{n\rm Q} \simeq A_{\rm Q\bar{Q}}/2 \simeq 0.12(1)$ for n=3,4,5. Therefore, the bare mass of diquark is expected to be simply considered as the twice of the quark mass.

In this paper, we consider two cases of the bare diquark mass. One is twice of constituent quark mass, i.e., $m_\phi = 600$ MeV. The other is twice of the running quark self-energy, i.e., $m_\phi(p_E^2) = 2\Sigma_q(p_E^2)$, where $\Sigma_q(p_E^2)$ is determined by the SD equation for single quark Eq. (4). This means that the diquark is constructed by the two dressing quarks. The constant bare mass case is based on the constituent quark model like picture and the running bare mass case is the SD formalism with omitting the effect of the gluonic attraction force between two quarks. The diquark should be dressed by gluon furthermore because of its non-zero color charge.

The cutoff Λ corresponds to the diquark size in a hadron, R, i.e., $\Lambda \equiv R^{-1}$, so the diquark should be smaller than the hadron. We also consider two cases of the size. One is the typical size of a baryon, $R=1$ fm, i.e., $\Lambda = 200$ MeV, which gives the upper limit of the size (the lower limit of the cutoff). The diquark covers the baryon in this case. The second is the typical size of a constituent quark, $R \simeq 0.3$ fm, i.e., $\Lambda = 600$ MeV, which gives the lower limit of the size (the upper limit of the cutoff).

4.2 The Constant Bare Mass Case

We first show in Fig. 6 the case of the constant bare mass $m_\phi = 600$ MeV with dependence on the cutoff Λ. The diquark self-energy $\Sigma(p^2)$ is always larger than the bare mass m_ϕ and almost constant except for a small bump structure at an infrared region. The value of the self-energy is strongly depends on the cutoff Λ, e.g., the "compact diquark" with $R \simeq 0.3$ fm has a large mass.

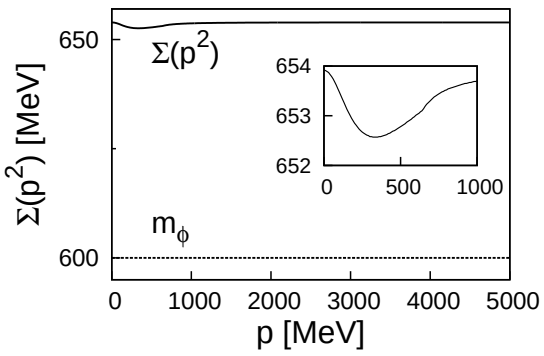

(a) $\Lambda = 200$ MeV ($R = 1$ fm)

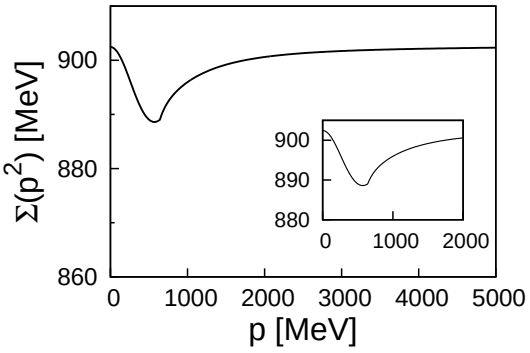

(b) $\Lambda = 600$ MeV ($R \simeq 0.3$ fm)

Fig. 6. The scalar diquark self-energy $\Sigma(p^2)$ as a function of the momentum p in the constant bare mass case of $m_\phi = 600$ MeV with (a) $\Lambda = 200$ MeV, i.e., $R = 1$ fm and (b) $\Lambda = 600$ MeV, i.e., $R \simeq 0.3$ fm. In both cases, there appears a small bump structure, which is displayed in the small window. In the left figure, the original bare mass m_ϕ is plotted for comparison.

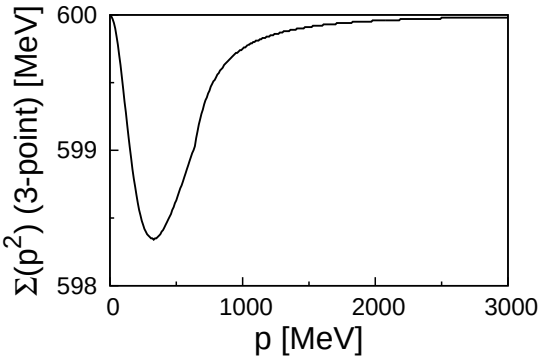

(a) Without 4-point interaction term

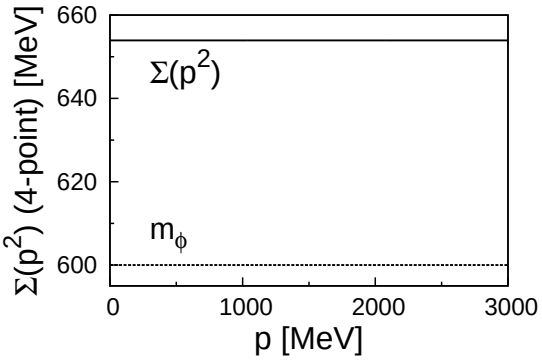

(b) Without 3-point interaction term

Fig. 7. The self-energy $\Sigma(p^2)$ in the case of (a) without 4-point interaction and (b) without 3-point interaction as the function of the momentum p. Here, $\Lambda = 200$ MeV is taken. In the right figure, the original bare mass m_ϕ is plotted for comparison.

The scalar QCD includes both 3-point and 4-point interactions, and the existence of 4-point interaction is diagrammatically different from the ordinary QCD. To see the role of each interaction, we consider the calculation of the artificial removal of 3-point interaction and 4-point interaction, respectively. In fact, we investigate the two cases: (a) removal of 4-point interaction and (b) removal of 3-point interaction. The result is shown in Fig. 7 in the case of $\Lambda = 200$ MeV. The bump structure appears in the case without the 4-point interaction term as shown in Fig. 7(a). Although the diagrammatic expression of the SD equation for the scalar diquark without 4-point interaction term is analogous to the quark SD equation, the behavior is completely different from the quark case. The diquark self-energy $\Sigma(p_E^2)$ starts from the bare mass $m_\phi = 600$ MeV at zero momentum, then decreases at low momentum and rises up to the original value 600 MeV. On the other hand, the quark self-energy $\Sigma_q(p_E^2)$ starts from a large value and goes to zero monotonously with the momentum. The SD equation without 3-point interaction just rises the self-energy and keeps constant. The strong dependence of the cutoff Λ (or the size R) mainly comes from the 4-point interaction term.

4.3 The Running Bare Mass Case

We show in Fig. 8 the case of the running bare mass $m_\phi(p_E^2) = 2\Sigma_q(p_E^2)$ with dependence on the cutoff Λ. The diquark self-energy $\Sigma(p_E^2)$ also strongly depends on the cutoff Λ. In the low-momentum region, the behavior of $\Sigma(p_E^2)$ reflects the running property of the bare mass, especially in the $\Lambda = 200$ MeV case, the gluonic effect seems to be small, because of $\Sigma(p_E^2) \approx 2\Sigma_q(p_E^2)$. In the high-momentum region, the diquark self-energy keeps a large value, while the bare mass $m_\phi(p_E^2)$ goes to zero. This suggests the mass generation of the scalar diquark by gluonic radiative correction.

4.4 Discussion on the Scalar Diquark Property

In this subsection, we discuss the mass and the size of the scalar diquark, with comparing to the chiral quark. One of the most important properties of single quark SD equation (4) is the existence of the trivial solution $\Sigma_q = 0$ in the chiral limit $m_q \to 0$. In fact, the quark mass remains to be zero due to the chiral symmetry in the perturbative treatment, and the quark mass generation, i.e., chiral symmetry breaking, is realized by the non-perturbative

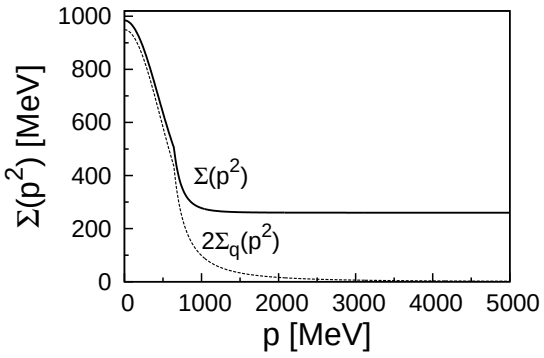

(a) $\Lambda = 200$ MeV ($R = 1$ fm)

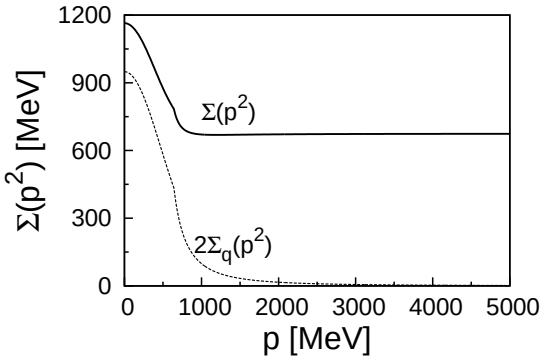

(b) $\Lambda = 600$ MeV ($R \simeq 0.3$ fm)

Fig. 8. The scalar diquark self-energy $\Sigma(p^2)$ as a function of the momentum p in the running bare mass case with (a) $\Lambda = 200$ MeV and (b) $\Lambda = 600$ MeV. The bare mass $m_\phi(p) = 2\Sigma_q(p)$ is also plotted with the dotted line for comparison.

gluonic interaction [63,64]. Such arguments can be done even in the limit of $\Lambda_{\rm UV} \to \infty$, which is consistent with the point quark as an elementary particle.

On the other hand, the SD equation (10) for scalar diquark has no trivial solution and is a highly non-linear equation, even in the zero bare mass limit $m_\phi \to 0$. For example, the 4-point interaction term gives a strong dependence of the UV cutoff Λ. This is similar to the framework of GUT, where the Higgs scalar field suffers from a large radiative correction of the GUT energy scale.

Actually, the scalar diquark self-energy $\Sigma(p^2)$ strongly depends on the diquark size $R \equiv \Lambda^{-1}$ in both cases of the bare mass. In an extreme case of the point-like limit $R \to 0$, i.e., $\Lambda \to \infty$, the diquark effective mass diverges. This suggests that the simple treatment of point-like diquarks is somehow dangerous in hadron models and the diquark must have an effective size.

As a quantitative argument, our calculations show that the "compact diquark" with $R \simeq 0.3$ fm has a large effective mass in both cases, and does not seem to be acceptable in effective models for hadrons. In fact, the appropriate diquark is not so compact as $R \simeq 0.3$ fm but is fairly extended as $R \sim 1$fm.

5 Mass Generation for Colored Scalar Particle

Finally, we consider the zero bare-mass case of diquark, $m_\phi \equiv 0$. Even for a finite mass of quark, the bare mass of diquark can be zero, if the attraction between two quarks extremely strong. The result is shown in Fig. 9 for the two cases: (a) $\Lambda = 200$ MeV and (b) $\Lambda = 600$ MeV on the cutoff. The self-energy $\Sigma(p_E^2)$ is always finite and takes a large value even for $m_\phi \equiv 0$. The mass generation mechanism in QCD is usually considered in the context of spontaneous chiral symmetry breaking. On the other hand, our scalar diquark theory is composed of an effective scalar diquark field $\phi(x)$ and does not have the chiral symmetry explicitly, although the original diquark is constructed by two chiral quarks. Nevertheless, the effective mass of diquark emerges by the non-perturbative gluonic effect. In fact, the mechanism of dynamical mass generation seems to work in the scalar diquark theory, even without chiral symmetry breaking. If we take $\Lambda = 1$ GeV, the diquark self-energy is $\Sigma \sim 950$ MeV. This result seems to be consistent with the lattice QCD result on the colored scalar particle [71].

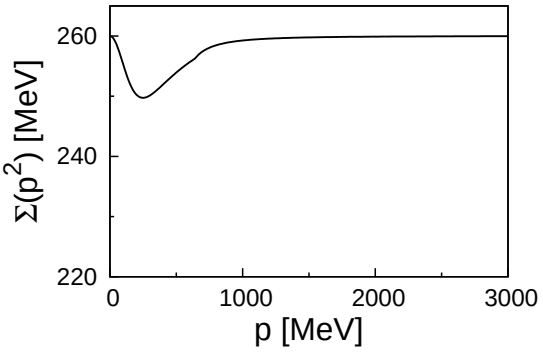

(a) $\Lambda = 200$ MeV ($R = 1$ fm)

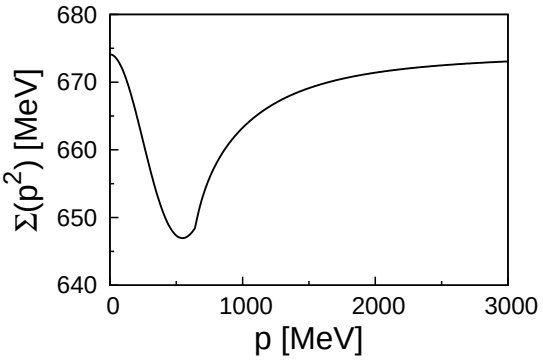

(b) $\Lambda = 600$ MeV ($R \simeq 0.3$ fm)

Fig. 9. The scalar diquark self-energy $\Sigma(p^2)$ as a function of the momentum p in the massless case of $m_\phi = 0$. The self-energy $\Sigma(p^2)$ is finite in both cases.

6 Conclusion and Discussion

We have investigated the gluonic effect to the scalar diquark, considering the size effect of the diquark in a hadron. The non-perturbative effect is evaluated in the Schwinger-Dyson (SD) formalism in the Landau gauge. The effect of diquark size is introduced as a cutoff parameter $\Lambda = R^{-1}$ in the form factor. We treat our theory as an effective cutoff theory.

The basic technology of scalar SD formalism is imported from the single quark case, such as the running coupling, the approximations and so on. Since the diquark is located in and construct of a hadron, the size should be smaller than the hadron ($R \sim 1$ fm) and larger than the constituent quark ($R \sim 0.3$ fm). The size (cutoff) dependence of self-energy have been investigated. We have considered the two cases of the constant bare mass $m_\phi = 600$ MeV and the running bare mass $m_\phi(p_E^2) = 2\Sigma_q(p_E^2)$. The diquark self-energy strongly depends on the size $R = \Lambda^{-1}$ in both cases, especially the small diquark ($R \simeq 0.3$ fm) has a large effective mass by the gluonic dressing effect.

We find that the effective diquark mass is finite and large even for the zero bare-mass case, and the value strongly depends on the size R, which is an example of dynamical mass generation by the gluonic effect, without chiral symmetry breaking. The mass difference between current and constituent charm quark mass and the large glueball mass are also examples of this type of mass generation. In this sense, the spontaneous chiral symmetry breaking may be a special case of massless (or small mass) fermion. It may be a general property of strong interacting theory that all colored particles acquire a large effective mass by the dressing effect as shown in Fig. 10.

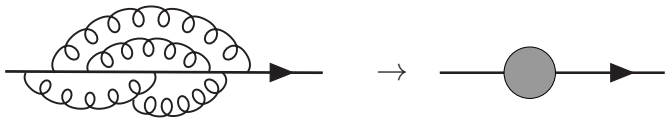

Fig. 10. The schematic picture for dynamical mass generation of the colored particle. The colored particle (solid line) interacting with the gluons (curly line). The effective mass emerges by the non-perturbative interaction even without the chiral symmetry.

In this study, we have mainly investigated the diquark properties, and have not calculated physical quantities. It is however desired to describe the color-singlet states such as heavy baryon Qqq based on the scalar theory. One of description of diquark based on QCD is the Bethe-Salpeter (BS) formalism for two quarks [91,92,93,94]. However, the treatment of the scalar diquark as an explicit degree of freedom $\phi(x)$ is a good approximation for the structure of the heavy baryons. The constituent scalar-quark(diquark)/quark picture in the scalar lattice QCD [71] and the structure of Λ_h ($h = s, c, b$ quarks) with explicit diquark degree of freedom using QCD sum rule [32] have been discussed. The description of the heavy baryon as heavy quark/diquark ($Q\phi$) using the BS equation will be investigated as our future work.

The tetra-quark states $qq\bar{q}\bar{q}$ may include diquark/antidiquark components. Although the two mesons molecular states may dominate in the tetra-quark due to the strong correlation between quark and antiquark, the diquark/antidiquark would be also important components [11,12,13,14,15]. The tetra-quark states would be described as the linear combination of two mesons and diquark/antidiquark states based on the BS formalism. The structure of sigma meson (light scalar mesons) is also applicable subject. The sigma meson is considered as a chiral partner of the pion in the context of the chiral symmetry, which structure is quark/antiquark bound state. The possibility of the light scalar mesons as four-quark states have been discussed [10,13,14,15,16,17,18,19,20,21,22,23,24,25]. The structure of the sigma meson (light scalar mesons) can be described as the linear combination of quark/antiquark, diquark/antidiquark and two mesons in the context of the BS formalism.

S.I. thanks T.M. Doi, H. Iida and N. Yamanaka for useful discussion and comments. This work is in part supported by the Grant for Scientific Research [Priority Areas "New Hadrons" (E01:21105006), (C) No.23540306, No.15K05076] from the Ministry of Education, Culture, Science and Technology (MEXT) of Japan

References

1. K.A. Olive et al. (Particle Data Group), Chin. Phys. C,**38**, 090001 (2014).
2. N. Brambilla et al., Eur. Phys. J. **C71**, 1534 (2011).
3. S. Cho et al. (ExHIC Collaboration), Phys. Rev. Lett. **106**, 212001 (2011).
4. D. Lichtenberg and L. Tassie, Phys. Rev. **155**, 1601 (1967).
5. M. Ida and R. Kobayashi, Prog. Theor. Phys. **36**, 846 (1966).
6. A. De Rujula, H. Georgi, and S. Glashow, Phys. Rev. **D12**, 147 (1975).
7. T. A. DeGrand, R. Jaffe, K. Johnson, and J. Kiskis, Phys. Rev. **D12**, 2060 (1975).
8. R. Jaffe, Phys. Rept. **409**, 1 (2005); Nucl. Phys. Proc. Suppl. **142**, 343 (2005).
9. F. Close, Int. J. Mod. Phys. **A20**, 5156 (2005).
10. R. L. Jaffe, Phys. Rev. **D15**, 267 (1977).
11. L. Maiani, F. Piccinini, A. Polosa, and V. Riquer, Phys. Rev. **D71**, 014028 (2005).
12. G.-J. Ding and M.-L. Yan, Phys. Lett. **B643**, 33 (2006).
13. A. Zhang, T. Huang, and T. Steele, Phys. Rev. **D76**, 036004 (2007).
14. H.-J. Lee, Eur. Phys. J. **A30**, 423 (2006).
15. W. Heupel, G. Eichmann, and C. S. Fischer, Phys. Lett. **B718**, 545 (2012).
16. M. G. Alford and R. Jaffe, Nucl. Phys. **B578**, 367 (2000).
17. H. Suganuma, K. Tsumura, N. Ishii and F. Okiharu, Prog. Theor. Phys. Suppl. **168**, 168 (2007).
18. S. Prelovsek, T. Draper, C. B. Lang, M. Limmer, K.-F. Liu, N. Mathur and D. Mohler, Phys. Rev. **D82**, 094507 (2010).

19. M. Wakayama et al. (SCALAR Collaboration), Phys. Rev. **D91**, 094508 (2015).
20. C. Alexandrou, J. O. Daldrop, M. D. Brida, M. Gravina, L. Scorzato, C. Urbach and M. Wagner, JHEP **1304**, 137 (2013).
21. H.-X. Chen, A. Hosaka and S.-L. Zhu, Phys. Rev. **D77**, 094025 (2007); Phys. Lett. **B650**, 369 (2007); Phys. Rev. **D74**, 054001 (2006).
22. H.-X. Chen, A. Hosaka, H. Toki and S.-L. Zhu, Phys. Rev. **D81**, 114034 (2010).
23. J. Sugiyama, T. Nakamura, N. Ishii, T. Nishikawa and M. Oka, Phys. Rev. **D76**, 114010 (2007).
24. A. H. Fariborz, R. Jora and J. Schechter, Phys. Rev. **D77**, 094004 (2008).
25. G. 't Hooft, G. Isidori, L. Maiani, A. Polosa, and V. Riquer, Phys. Lett. **B662**, 424 (2008).
26. J. L. Rosner, Phys. Rev. **D75**, 013009 (2007).
27. X.-H. Guo, A. W. Thomas, and A. G. Williams, Phys. Rev. **D59**, 116007 (1999).
28. M.-H. Weng, X.-H. Guo, and A. Thomas, Phys. Rev. **D83**, 056006 (2011).
29. T. Mehen and B. C. Tiburzi, Phys. Rev. **D74**, 054505 (2006).
30. A. Selem and F. Wilczek, arXiv:hep-ph/0602128.
31. E. Hernandez, J. Nieves, and J. Verde-Velasco, Phys. Lett. **B666**, 150 (2008).
32. K. Kim, D. Jido, and S. H. Lee, Phys. Rev. **C84**, 025204 (2011); Few Body Syst. **54** 271 (2013).
33. A. Martynenko and V. Saleev, Phys. Lett. **B385**, 297 (1996).
34. M. Gomshi Nobary and R. Sepahvand, Phys. Rev. **D76**, 114006 (2007).
35. D. Ebert, T. Feldmann, C. Kettner, and H. Reinhardt, Int. J. Mod. Phys. **A13**, 1091 (1998); D. Ebert, R. Faustov, and V. Galkin, Phys. Rev. **D84**, 014025 (2011).
36. R. L. Jaffe and F. Wilczek, Phys. Rev. Lett. **91**, 232003 (2003).
37. S. H. Lee and S. Yasui, Eur. Phys. J. **C64**, 283 (2009); S. H. Lee, S. Yasui, W. Liu, and C. M. Ko, Eur. Phys. J. **C54**, 259 (2008).
38. E. Shuryak and I. Zahed, Phys. Lett. **B589**, 21 (2004).
39. D. K. Hong, Y. J. Sohn, and I. Zahed, Phys. Lett. **B596**, 191 (2004).
40. M. Karliner and H. J. Lipkin, Phys. Lett. **B575**, 249 (2003).
41. T. Hyodo, Y.-R. Liu, M. Oka, K. Sudoh and S. Yasui, Phys. Lett. **B721**, 56 (2013).
42. S. Yasui and M. Oka, Phys. Rev. **D76**, 034009 (2007).
43. A. Bacchetta, F. Conti, and M. Radici, Phys. Rev. **D78**, 074010 (2008).
44. D. Lichtenberg, W. Namgung, E. Predazzi, and J. Wills, Phys. Rev. Lett. **48**, 1653 (1982).
45. J. Ferretti, A. Vassallo, and E. Santopinto, Phys. Rev. **C83**, 065204 (2011).
46. K. Nagata and A. Hosaka, Prog. Theor. Phys. **111**, 857 (2004).
47. S. Fredriksson, M. Jandel, and T. Larsson, Z. Phys. **C14**, 35 (1982).
48. C. Alexandrou, P. de Forcrand, and B. Lucini, Phys. Rev. Lett. **97**, 222002 (2006).
49. R. Babich et al., Phys. Rev. **D76**, 074021 (2007).
50. T. DeGrand, Z. Liu, and S. Schaefer, Phys. Rev. **D77**, 034505 (2008).
51. M. Hess, F. Karsch, E. Laermann, and I. Wetzorke, Phys. Rev. **D58**, 111502 (1998).
52. M. G. Alford, A. Schmitt, K. Rajagopal, and T. Schäfer, Rev. Mod. Phys. **80**, 1455 (2008).
53. S. Imai, H. Toki, and W. Weise, Nucl. Phys. **A913**, 71 (2013).
54. C. Ratti and W. Weise, Phys. Rev. D **70**, 054013 (2004).
55. M. Harada, C. Nonaka, and T. Yamaoka, Phys. Rev. **D81**, 096003 (2010).
56. K. Splittorff, D. Toublan, and J. Verbaarschot, Nucl.Phys. **B620**, 290 (2002).
57. S. Hands, S. Kim, and J.-I. Skullerud, Eur. Phys. J. **A31**, 787 (2007).
58. J. B. Kogut, D. Toublan, and D. K. Sinclair, Phys. Lett. **B514**, 77 (2001).
59. N. Strodthoff, B.-J. Schaefer, and L. von Smekal, Phys. Rev. **D85**, 074007 (2012).
60. R. Alkofer and L. von Smekal, Phys. Rept. **353**, 281 (2001).
61. P. Maris and C. D. Roberts, Int. J. Mod. Phys. **E12**, 297 (2003).
62. C. D. Roberts and A. G. Williams, Prog. Part. Nucl. Phys. **33**, 477 (1994).
63. V. A. Miransky, Sov. J. Nucl. Phys. **38**, 280 (1983); *Dynamical Symmetry Breaking in Quantum Field Theories*, World Sicentific, Singapore, 1994.
64. K. Higashijima, Phys. Rev. **D29**, 1228 (1984); Prog. Theor. Phys. Suppl. **104**, 1 (1991)
65. K.-I. Aoki, M. Bando, T. Kugo, M. G. Mitchard, and H. Nakatani, Prog. Theor. Phys. **84**, 683 (1990).
66. T. Kugo and M. G. Mitchard, Phys. Lett. **B286**, 355 (1992).
67. C. S. Fischer, J. Phys. **G32**, R253 (2006).
68. H. Munczek, Phys. Rev. **D52**, 4736 (1995).
69. N. Yamanaka, T. M. Doi, S. Imai, and H. Suganuma, Phys. Rev. **D88**, 074036 (2013); N. Yamanaka, S. Imai, T. M. Doi, and H. Suganuma, Phys. Rev. **D89**, 074017 (2014).
70. S. Imai and H. Suganuma, PoS Hadron2013, 148 (2014), arXiv:1401.3099 [hep-ph]
71. H. Iida, H. Suganuma, and T.T. Takahashi, Phys. Rev. **D75**, 114503 (2007); Mod. Phys. Lett. **A23**, 2344 (2008); AIP Conf. Proc. **915**, 256 (2007).
72. T.-P. Cheng and L.-F. Li, *Gauge Theory of Elementary Particle Physics*, Oxford University Press, U.S.A., 1988.
73. M. E. Peskin and D. V. Schroeder, *An Introduction To Quantum Field Theory (Frontiers in Physics)*, Westview Press, 1995.
74. G. Aad et. al (ATLAS Collaboration), Phys. Lett. **B716**, 1 (2012).
75. A. Maas, Eur. Phys. J. **C71**, 1548 (2011); PoS FACESQCD, 033 (2010), arXiv:1102.0901 [hep-lat]; A. Maas and T. Mufti, JHEP **1404**, 006 (2014).
76. V. Macher, A. Maas and R. Alkofer, Int. J. Mod. Phys. A **27**, 1250098 (2012).
77. M. Hopfer and R. Alkofer, Acta Phys. Polon. Supp. **6**, 929 (2013).
78. T. Iritani, H. Suganuma, and H. Iida, Phys. Rev. **D80**, 114505 (2009).
79. J. Mandula and M. Ogilvie, Phys. Lett. **B185**, 127 (1987).
80. K. Amemiya and H. Suganuma, Phys. Rev. **D60**, 114509 (1999).
81. C. J. Morningstar and M. J. Peardon, Phys. Rev. **D60**, 034509 (1999).

82. N. Ishii, H. Suganuma, and H. Matsufuru, Phys. Rev. **D66**, 094506 (2002).
83. Y. Nambu and G. Jona-Lasinio, Phys. Rev. **122**, 345 (1961).
84. T. Hatsuda and T. Kunihiro, Phys. Rept. **247**, 221 (1994).
85. H. Pagels and S. Stokar, Phys. Rev. **D20**, 2947 (1979).
86. G. 't Hooft, Phys. Rev. **D14**, 3432 (1976).
87. T. Schäfer and E. V. Shuryak, Rev. Mod. Phys. **70**, 323 (1998).
88. C. Itzykson, J.-B. Zuber, *Quantum Field Theory*, Dover Publications, 2006.
89. J. Marinho, E. Gambin, and T. Frederico, AIP Conf.Proc. **884**, 378 (2007).
90. A. Salam and J. Strathdee, Phys. Rev. **D18**, 4713 (1978).
91. A. Bender, C. D. Roberts, and L. Von Smekal, Phys. Lett. **B380**, 7 (1996).
92. R. Cahill, C. D. Roberts, and J. Praschifka, Phys. Rev. **D36**, 2804 (1987).
93. Z. Wang, S. Wan, and W. Yang, Commun. Theor. Phys. **47**, 287 (2007).
94. J. C. Bloch, C. D. Roberts, S. Schmidt, A. Bender, and M. Frank, Phys. Rev. **C60**, 062201 (1999); J. C. Bloch, C. D. Roberts, and S. Schmidt, Phys. Rev. **C60**, 065208 (1999).
95. T. T. Takahashi, H. Matsufuru, Y. Nemoto, and H. Suganuma, Phys. Rev. Lett. **86**, 18 (2001); T. T. Takahashi, H. Suganuma, Y. Nemoto, and H. Matsufuru, Phys. Rev. **D65**, 114509 (2002); N. Sakumichi and H. Suganuma, Phys. Rev. **D92**, 034511 (2015).
96. F. Okiharu, H. Suganuma, and T. T. Takahashi, Phys. Rev. Lett. **94**, 192001 (2005); Phys. Rev. **D72**, 014505 (2005).